

pubs.acs.org/crystal Article

# A New Software Framework for Implementing Crystal Growth Models to Materials of Any Crystallographic Complexity

Yongsheng Zhao, Carl J. Tilbury, Steven Landis, Yuanyuan Sun, Jinjin Li, Peng Zhu, and Michael F. Doherty\*



Cite This: Cryst. Growth Des. 2020, 20, 2885–2892



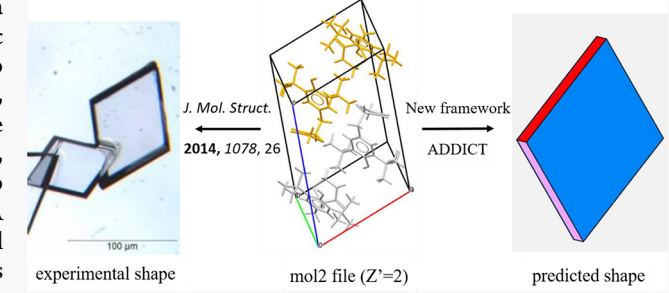
**ACCESS** 

Metrics & More

Article Recommendations

Supporting Information

ABSTRACT: To continue the realization of new therapeutics, a more diverse range of solid forms is being considered. Synthetic modalities are broadening beyond simple organic molecules to more complicated structures, including organic salts, cocrystals, and solvates. As in all crystalline applications, engineering the morphology of such systems remains an important consideration, but traditional in silico approaches require further development to become capable of accurately describing these systems. A necessary, but not sufficient, condition to enact mechanistic crystal growth models is to calculate and organize solid-state interactions between growth units. The typical software framework for



acquiring this information is to apply crystallographic symmetry operations to generate a unit cell from the asymmetric unit. While this approach is feasible for systems where the asymmetric unit corresponds to the growth unit itself, many systems do not satisfy this criterion, particularly the emerging therapeutic solid forms. By redesigning the input preparation software framework, we can build a description of the solid-state interactions that is independent of the asymmetric unit and applicable to any crystallographic complexity. We demonstrate the application of this method to three organic molecular crystals with crystallography of varying degrees of complexicty. The studied systems are naphthalene (Z' = 0.5), benzoic acid (Z' = 1), and tazofelone (Z' = 2), respectively (where Z' is the number of molecules in the asymmetric unit). This new software framework lays the groundwork for rapid in silico habit predictions of organic salts, cocrystals, and solvates.

# **■** INTRODUCTION

Engineering the shape of crystals is critical to achieve material properties that confer optimal product functionality. 1-5 In silico methods that can predict crystal growth shapes are a valuable tool for efficiently navigating the large design space of growth conditions. Such tools can guide experiments and enable cheaper and more effective screening. However, industrially relevant compounds and complex solid forms require accurate models to properly account for the underlying chemistry and physics of crystal growth. To this end, mechanistic models are particularly useful, because any modeling assumptions that are inaccurate for such complex compounds can be systematically addressed via new procedures or equations that better capture the underlying crystal growth process. Experiments have readily established that crystal growth at low supersaturation, which is typical of controlled pharmaceutical crystallization, typically leads to the spiral mechanism of Frank and co-workers.<sup>6</sup> Our group at the University of California Santa Barbara (UCSB)<sup>7-9</sup> and the Koo group at Sogang University<sup>10-12</sup> have been developing and upgrading a mechanistic framework for modeling such surface growth physics for general, non-centrosymmetric compounds. A prerequisite of implementing such a mechanistic framework is the ability to categorize the solid-state interactions between growth units in the crystal.

An emerging aspect of the increasing complexity of industrial crystalline products is the crystallography itself, specifically the relation between the crystalline asymmetric unit (the asymmetric unit is the smallest part of a crystal structure to which symmetry operations can be applied to generate the complete unit cell) and the physical growth unit. Complex compounds may have more than one molecule within the asymmetric unit;  $^{13}$  solid forms such as hydrates, solvates, cocrystals, and organic salts must also have multiple molecules or chemical entities within the asymmetric unit. Such complex solid forms where Z' (the number of molecules in the asymmetric unit) does not equal unity are being more commonly introduced as techniques to optimize material properties and crystal shape.  $^{14-17}$  However, model compounds

Received: August 17, 2019 Revised: January 31, 2020 Published: March 11, 2020





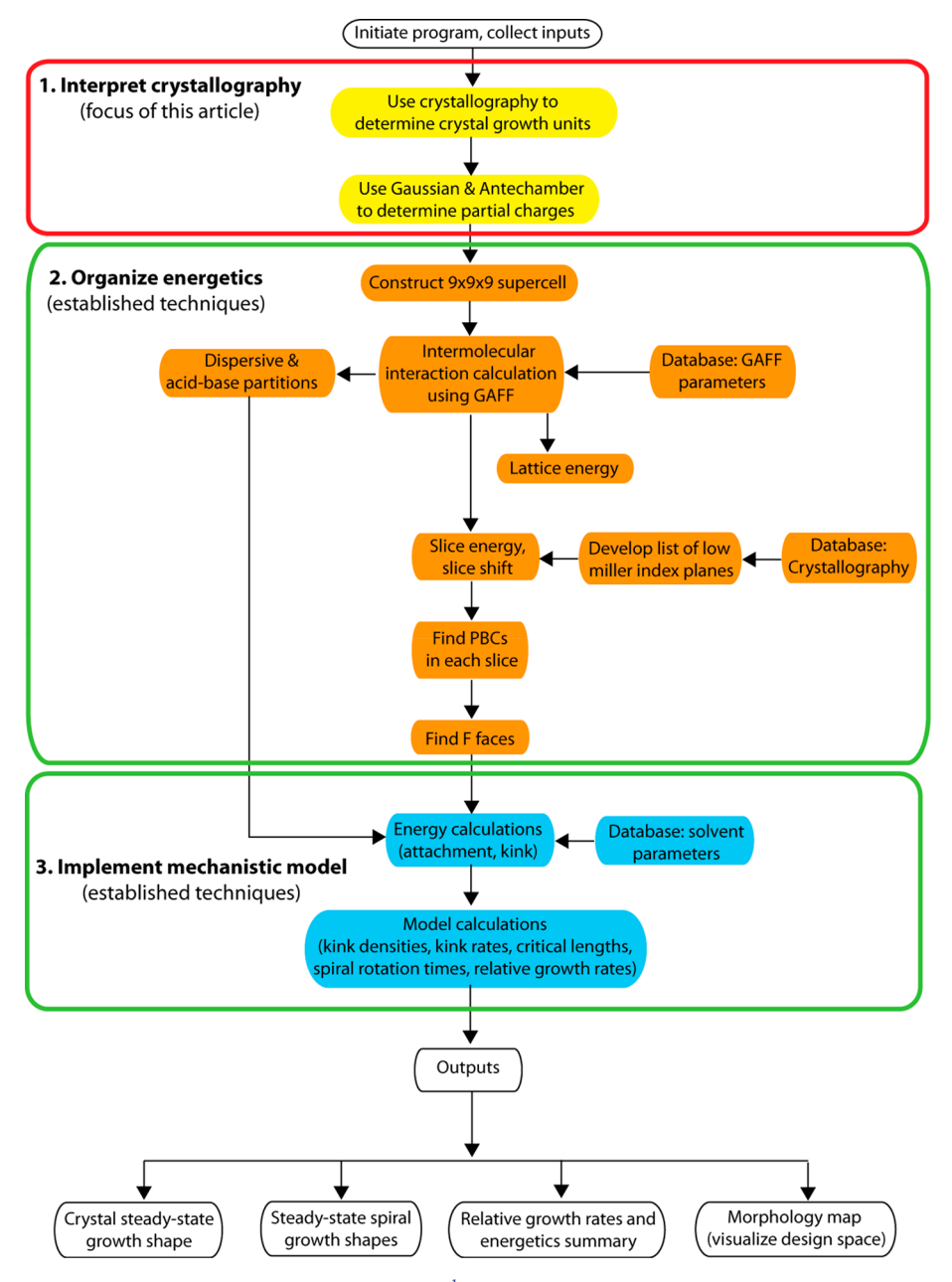


Figure 1. Overall mechanistic modeling framework within ADDICT. 1

studied from the perspective of mechanistic morphology predictions have typically been limited to a single molecule in the asymmetric unit. 18

As we describe in the next section, the traditional approach of obtaining solid-state interactions between growth units relies on determining the relationship between the crystal asymmetric unit and physical growth unit, which is nontrivial for more complex solid forms. In this article, we describe a new front-end software framework for the mechanistic framework, which is able to deal with any crystallographic complexity. Importantly, this software framework can determine solid-state interactions between all growth units in the lattice, regardless of how many molecular entities exist and what their relation is to the asymmetric unit (i.e., it is applicable to both Z'=1 and  $Z'\neq 1$ ). Furthermore, we also show how this approach can describe dimeric growth units, where the total intergrowth-unit

interaction must include each pairing of molecules between dimers.

# ■ OVERALL MECHANISTIC FRAMEWORK: ADDICT

Advanced Design and Development of Industrial Crystallization Technology (ADDICT) is a computer program that executes an automated implementation of mechanistic crystal growth models to predict and engineer crystal growth shapes, currently focusing on the layer-by-layer growth mechanisms of spiral growth and two-dimensional (2D) nucleation and growth. This provides a technology platform for transferring high-fidelity mechanistic growth models to researchers in industry, facilitating the adoption of these techniques.

The overall software framework and operation of ADDICT has been described previously. Figure 1 provides an updated overview of the overall software framework, which can be divided into three primary functions:

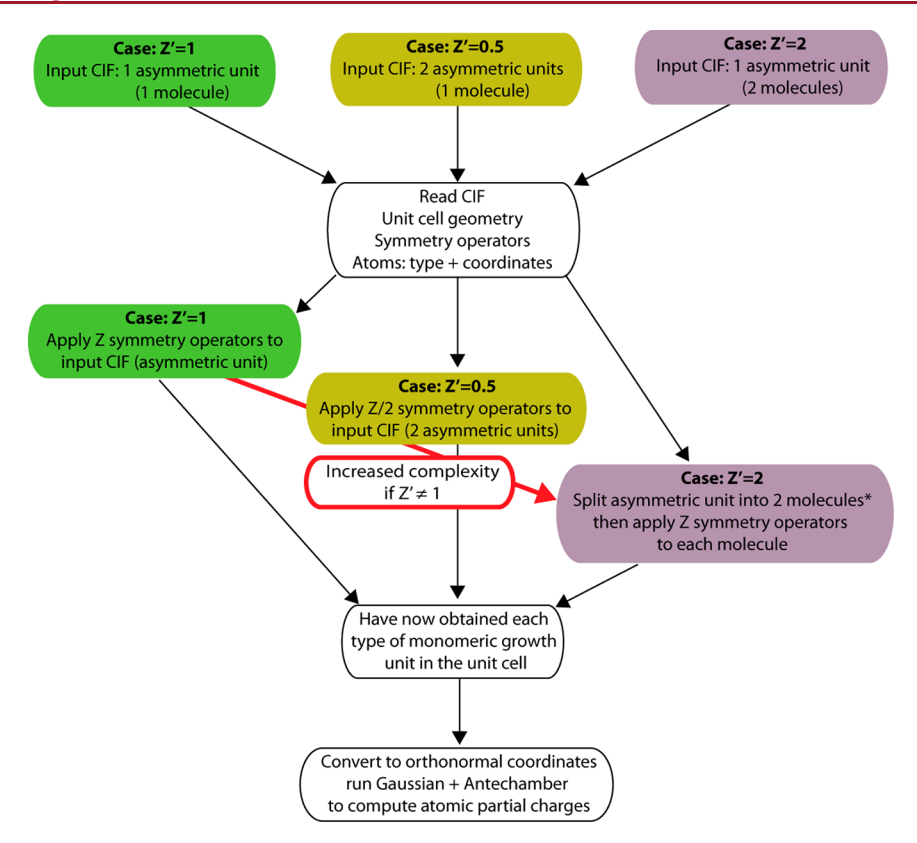


Figure 2. Traditional case-by-case software framework for determining physical growth units from input crystallography. \*Note that CIF files do not associate atoms with molecules. Thus, splitting the asymmetric unit into two molecules is complicated, as the CIF file does not require any systematic ordering of atoms and does not contain any markers to facilitate this decomposition.

- 1. Interpret Crystallography. ADDICT generates morphology predictions for a specific crystal polymorph, so the crystallography is a required input for the program. Crystals grow via incorporation of growth units into the lattice, and the mechanistic implementation (section 3) depends on the solid-state and interfacial interactions between growth units. Before such energetics are calculated, the growth units within the lattice must be systematically organized and determined.
- 2. Organize Energetics. With each growth unit in the crystal unit cell defined, solid-state interactions between growth units can be calculated. We use the Generalized Amber Force Field (GAFF 1.8) to calculate solid-state energy interactions. Accounting for each type of solid-state interaction enables calculation of the crystal lattice energy. Implementing the mechanistic models in Section 3 further requires energetics ordered around the relevant crystalline faces and favorable step-edge directions. Thus, another function of Section 2 is to develop a list of relevant crystal planes for the space group and determine the strong periodic bond chains that exist in each slice.
- **3. Implement Mechanistic Growth Model.** With faces determined and interactions organized around the strong solid-state energetic directions, mechanistic energies (e.g., kink energies, edge energies, etc.) can be established, including solution-growth modification. Established mechanistic equations <sup>7,8,19,21</sup> are applied to predict relative growth rates and calculate crystal growth habits, under the specified growth conditions.

The main focus of this article is a new procedure to implement Section 1 of this framework, which requires

generalizing in order to handle more complex solid forms (multiple molecules in asymmetric unit, cocrystals, hydrates, etc.). The next sections describe the previous and refined strategies for determining growth units and arriving at the point where Section 2 can calculate intergrowth-unit solid-state interactions and proceed with the remainder of the framework.

# PREVIOUS SOFTWARE FRAMEWORK FOR CRYSTALLOGRAPHY INTERPRETATION

The prior formulation for crystallography interpretation operated under the implicit assumption that the physical growth unit corresponded to either one or two asymmetric units. The case of two asymmetric units representing the growth unit corresponds to a centrosymmetric molecule for which the asymmetric unit is half a molecule. In essence, the framework required specific cases to be applicable.

Figure 2 indicates the previous software framework. If the asymmetric unit does correspond to a single growth unit (Z'=1), all other growth units in the unit cell can be generated by applying each symmetry operator (for the polymorph's space group) to the asymmetric unit. This produces each type of lattice growth unit, and Section 2 of the overall framework in Figure 1 can proceed with calculating solid-state interactions (via cycling through unit cell translations and each type of growth unit in both origin and destination unit cells).

If the asymmetric unit corresponds to half the molecule, to produce a growth unit one has two options. First, one could request a crystallography file (e.g., CIF file) containing the full molecule and then apply half of the symmetry operators (being careful that each symmetry operator applied actually does produce a new growth unit rather than mapping to an existing

one). Second, one could operate on the asymmetric unit (e.g., applying an inversion center for centrosymmetric molecules) to first produce the growth unit, and then continue as usual in applying only half of the relevant symmetry operators remaining.

It should be apparent that the above tactics are not satisfactory for an automated procedure, and it becomes even more difficult for  $Z' \geq 2$ . This prior software framework necessitates user expertise to appropriately format the supplied crystallography and inform which symmetry operators are relevant and how the asymmetric unit relates to the growth unit. To implement such a software framework for more complex systems without a significant burden on users would require extensive redundancy built into the code to recognize symmetry operators that map onto each other and where solid-state distances are such that two asymmetric units must belong to the same molecule.

Figure A1 in Appendix A in the Supporting Information provides various crystallographic unit cell examples, and Table A1 in Appendix A in the Supporting Information provides connections between molecules, asymmetric units, symmetry operators, and growth units for the crystallographic examples in Figure A1.

# NEW SOFTWARE FRAMEWORK FOR CRYSTALLOGRAPHY INTERPRETATION

The fundamental change in the new proposed software framework is to start with the entire unit cell, rather than the asymmetric unit, and to utilize the MOL2 file format. The MOL2 file labels each atom according to which chemical entity within the unit cell contains it (i.e., which organic molecule, which salt ion, etc.). Thus, by reading in this information, each type of monomeric crystal growth unit within the lattice can be readily identified, along with all atoms contained and their individual atom types and spatial coordinates. Furthermore, this preparation step is easy to implement using Mercury, <sup>22</sup> so it does not require specialized expertise in crystallography to produce. The CIF file becomes an additional input, but instead of reading atomic positions, the CIF file is merely used to obtain the crystallographic dimensions, symmetry operators, and space group.

The number of molecules in the unit cell (Z) can be counted directly using the unit cell MOL2 file. However, care must be taken to define a unique unit cell and remove molecules that are repeated in the a,b,c directions (such molecules have a center of mass exactly on the unit cell surface). The number of molecules in the asymmetric unit (Z') can be calculated by dividing Z by the number of symmetry operators. Note that the CIF file contains no natural identification of Z', which is why the previous case-by-case interpretation introduced significant difficulties for more complex crystallography.

As described previously, partial charges are required for all atoms to calculate solid-state interactions; we use ANTE-CHAMBER<sup>23</sup> on top of a Gaussian<sup>24</sup> calculation to determine these partial charges. A Gaussian calculation is required for each distinct molecule in the lattice. Since this new software framework readily identifies each molecule within the unit cell, Gaussian input files can be generated for each type of molecule (this is a critical generalization for cases when more than one type of molecule exists, e.g., for cocrystals or solvates).

Figure 3 illustrates this new software framework for crystallography interpretation, which facilitates determination of solid-state intergrowth-unit interactions (the downstream

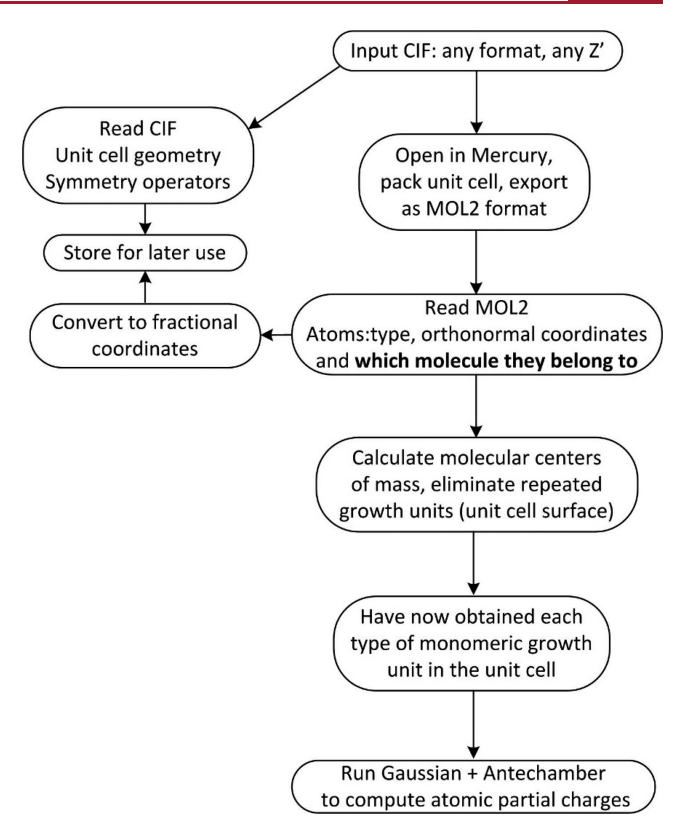


Figure 3. New general software framework for crystallography interpretation.

mechanistic framework in Figure 1 remains essentially unmodified).

If the crystal grows as a dimer, further steps are required to produce the dimeric growth unit from the monomers that have been identified thus far. The first step involves selecting the pair of molecules to form the dimer. Either the largest solid-state intermolecular interaction strength, or the shortest intermolecular interaction distance, represent potential techniques to determine the most probable dimer. Experimental evidence may also be used to select the molecular pair that corresponds to the dimer (see Appendix B in Supporting Information).

Once the dimer growth unit has been identified, intergrowth-unit interactions (i.e., between dimers) can then be produced by summing all interatomic interactions between each atom of dimer No. 1 and each atom of dimer No. 2. The intradimer intermolecular interaction is no longer included as part of the solid-state lattice energy, since dimers remain intact in the growth medium.

# **■** RESULTS: CASE STUDY

We chose three systems, which have Z'=0.5, Z'=1, and Z'=2, respectively, to demonstrate application of mechanistic crystal growth models to cases with crystallography of varying degrees of complexicty. The studied systems are naphthalene (Z'=0.5), benzoic acid (Z'=1), and tazofelone (Z'=2). In this study, only the molecule–molecule bonds for which  $|E| \geq 0.3$  kcal/mol ( $\sim 0.5$  kT at room temperature) are included; for organic molecules this energy threshold is sufficient to reflect the dominant interactions between different growth units within the supercell.

Naphthalene (Cambridge Structural Database (CSD) CIF code NAPHTA10<sup>2.5</sup>) is a simple centrosymmetric crystal and crystallizes in the monoclinic  $P2_1/a$  space group with half a molecule in the asymmetric unit and two molecules in the unit cell (Z' = 0.5, Z = 2). The cell parameters of naphthalene are a = 8.2128 Å; b = 5.9727 Å; c = 8.6745 Å;  $\alpha = \gamma = 90^{\circ}$ ; and  $\beta = 123.388^{\circ}$ . The growth unit that incorporates into kink sites is the monomer molecule.

After appropriately interpreting the crystallography for naphthalene according to the flow in Figure 3 (see Appendix C in Supporting Information for the step-by-step implementation), interactions were calculated using the Generalized Amber Force Field<sup>26</sup> and RESP charges following an Antechamber<sup>23</sup> calculation. Accounting for the molecular interaction energetics is critical to the mechanistic model, and the presence of a solvent alters the relevant surface interactions due to solvation of the crystal surface.<sup>20</sup> Therefore, different solvents can have different effects on the crystal surface, resulting in different crystal facets having different growth rates. The specific details of how the solvent affects the interfacial interactions and the calculation of solute—solvent interfacial energies can be found in the Supporting Information. As shown in Figure 4, the predicted crystal

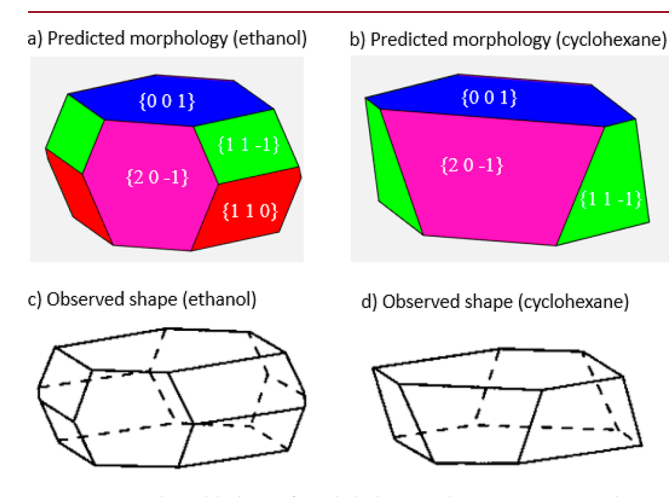


Figure 4. Predicted habits of naphthalene with monomer growth unit grown from ethanol (a) and grown from cyclohexane (b) using the vOCG solvent model; the experimental shapes of naphthalene grown from ethanol (c) and grown from cyclohexane (d).

morphologies of naphthalene monomer growth from ethanol (S = 1.04, T = 298 K) and from cyclohexane (S = 1.01, T =298 K) using the van Oss, Chaudhury, & Good (vOCG) solvent model<sup>20</sup> (also see the Supporting Information) are in good agreement with the experimental shapes.<sup>27</sup> The periodic bond chains (PBCs), spiral shapes, and detailed calculated results of naphthalene can be found in the Supporting Information. Dimer growth was also used to predict crystal morphologies of naphthalene grown from ethanol and from cyclohexane solvents at the same growth conditions as for monomer growth. As shown in Figure 5, the predicted crystal morphologies of naphthalene are inconsistent with the experimental morphologies, indicating that the growth unit is a monomer not a dimer. Therefore, it is very important to correctly select the type of growth unit. Some of the rules and details on how to select monomer or dimer crystal growth can be found in Appendix B in the Supporting Information.

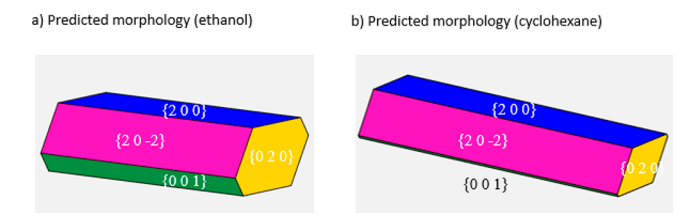
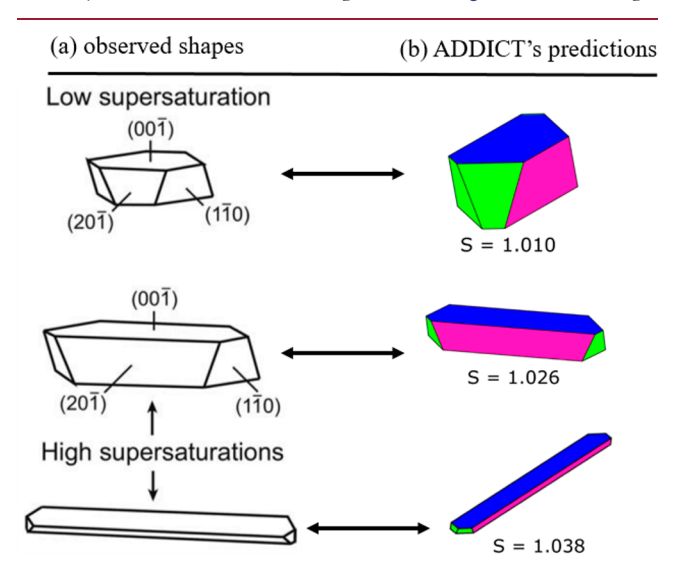


Figure 5. Predicted habits of naphthalene with dimer growth unit grown from ethanol (a) and grown from cyclohexane (b) using the vOCG solvent model.

Using ADDICT we also calculated the change in shape with increasing levels of supersaturation for naphthalene grown from cyclohexane. These are reported in Figure 6. The shape



**Figure 6.** Change in experimental (a) $^{19,27,28}$  and predicted (b) shapes with increasing levels of supersaturation for naphthalene grown from cyclohexane using the vOCG solvent model.

changes are due to a change in growth mechanism from spiral growth to 2D birth and spread and 2D polynuclear as supersaturation increases. The predicted shape changes are in good agreement with experiment. Note that simpler growth models such as the Bravais, Friedel, Donnay, and Harker  $(BFDH)^{29-31}$  and attachment energy  $(AE)^{32}$  models are incapable of predicting crystal shape changes that result from changes in supersaturation.

Benzoic acid ( $C_7H_6O_2$ , commonly used as a drug or preservative) was modeled using CSD CIF code BENZAC02.<sup>33</sup> Benzoic acid crystallizes in the monoclinic  $P2_1/c$  space group with one (non-centrosymmetric) benzoic acid molecule in the asymmetric unit and four benzoic acid molecules in the unit cell (Z'=1, Z=4). The cell parameters of benzoic acid are a=5.4996 Å; b=5.1283 Å; c=21.950 Å;  $\alpha=\gamma=90^\circ$ ; and  $\beta=97.37^\circ$ .

According to Appendix B in the Supporting Information, since the H atom in the hydroxyl group of one benzoic acid molecule has a strong hydrogen bond with the oxygen atom of another benzoic acid (and vice versa), dimer growth was used to predict the crystal morphology of benzoic acid crystal grown from the vapor phase. Organizing those interactions between dimer growth units (centrosymmetric) revealed four relevant families of F faces,  $^{24}$  namely,  $\{1\ 0\ -2\}$ ,  $\{1\ 0\ 0\}$ , and  $\{0\ 1\ 1\}$ . Figure 7a illustrates the predicted vapor growth shape for

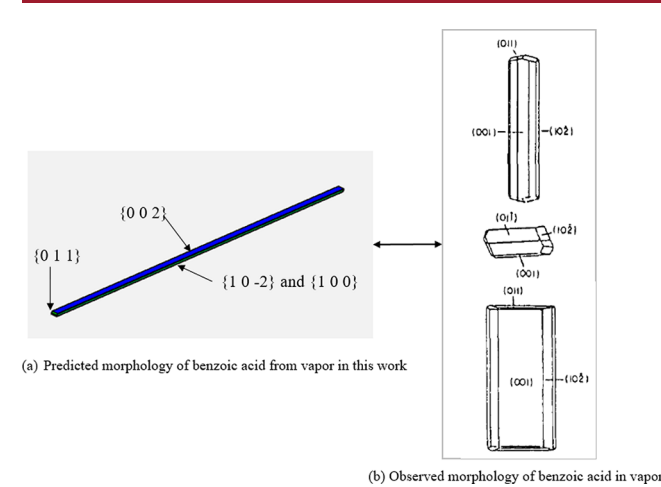


**Figure 7.** Views of the predicted habit of benzoic acid grown from vapor (a) and the experimental vapor morphology as viewed along the a, b, and c axes (from top to bottom, respectively) (b)<sup>34</sup>

benzoic acid crystals that results from spiral growth on these F faces. Figure 7b indicates the experimentally observed crystal morphology as viewed along the a, b, and c axes.<sup>34</sup> It can be seen from Figure 7 that the Miller indices of the F faces we predicted are exactly the same as those reported in the literature.<sup>34</sup> However, the predicted growth rate of the {0 1 1} face family is much larger than the experimental value, so that the shape of benzoic acid we predicted is a needle. By carefully analyzing the PBCs of the {0 1 1} and {0 0 2} face families, we can be sure that the growth rate of the former is ~183 times that of the latter (S = 1.04, T = 298 K), and the experimental crystal shape of benzoic acid should be needlelike (see Supporting Information). Since it is difficult to find experimental results in the literature on benzoic acid crystallization from the vapor, we searched for other sources. We found a video on YouTube that confirms our predictions.<sup>35</sup> This video shows a laboratory demonstration of the purification of benzoic acid by sublimation, which clearly shows that needle-shaped crystals of benzoic acid are obtained by sublimation growth. Since the needle-shaped crystal is very fragile, we hypothesize that, perhaps in the literature, <sup>34</sup> only a part of the sample that has been broken was used for characterization, thereby obtaining a non-needle crystal shape. The PBCs, spiral shapes, and detailed calculated results of benzoic acid can be found in the Supporting Information.

The final system we report is tazofelone form III (CSD CIF code WIMBAV13<sup>36</sup>), grown from toluene. Tazofelone is a potent antioxidant and 5-lipoxygenase inhibitor, which was originally investigated at Eli Lilly two decades ago as a novel therapy for inflammatory bowel diseases.<sup>36</sup> Tazofelone form III crystallizes in the space group  $P\overline{1}$  with the following cell parameters: a = 11.2917 Å; b = 11.9167 Å; c = 14.9597 Å; and  $\alpha = 77.827^{\circ}$ ;  $\beta = 75.208^{\circ}$ ;  $\gamma = 71.585^{\circ}$ . There are two molecules in the asymmetric unit and four molecules in the unit cell (Z' = 2, Z = 4). According to Appendix B in the Supporting Information, due to the formation of two strong N-H···O hydrogen bonds between two tazofelone molecules (-19.16 kcal/mol, calculated using the GAFF force field in ADDICT), a dimer growth unit was used to predict the crystal morphology of tazofelone crystals grown from toluene solvent. The original unit cell (monomer growth) and the new unit cell formed based on the dimer growth unit can be found in the Supporting Information. Figure 8a indicates the predicted

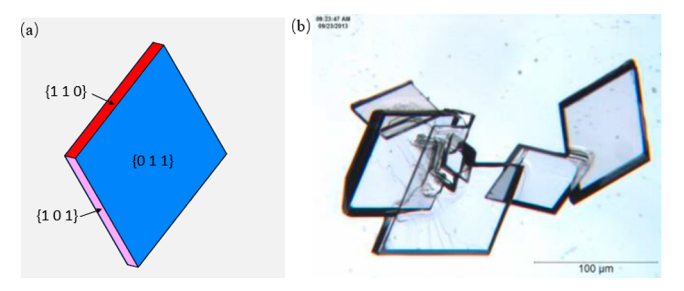


**Figure 8.** Views of the predicted shape of tazofelone grown from toluene using the vOCG solvent model (a) and the experimental shape grown from toluene  $(b)^{36}$ 

crystal shapes of tazofelone (S=1.04, T=298 K) grown from toluene using the vOCG solvent model. The experimental shape of tazofelone form III grown from toluene has been reported, for producing crystals with shapes shown in Figure 8b; while the Miller index faces of the experimental crystals are unknown, our theoretical morphologies do indicate similar parallelogram shapes. The PBCs, spiral shapes, and calculation results of tazofelone can be found in the Supporting Information. In addition, note that, as far as we are aware, this is the first time that the crystal morphology for a Z'=2 crystal was successfully predicted using the mechanistic growth model. To further prove the reliability of our new software framework, we also predicted the morphology of 4-hydroxyacetophenone crystal with Z'=2. The specific results are shown in the Supporting Information.

## CONCLUSIONS

When the crystallographic asymmetric unit is not equal to a single growth unit, it is more challenging to implement mechanistic models of crystal growth. Furthermore, the relationship between the asymmetric unit and the growth unit requires a case-by-case treatment that makes an automated model implementation especially challenging. To resolve this disconnect, we propose adjusting the input crystallographic information for mechanistic models to be the full unit cell, stored in an MOL2 file format. This has the significant advantage of identifying which molecule or chemical entity each atom belongs to, automatically producing all types of monomeric crystal growth unit for a given system. Thus, the growth algorithms can interpret the crystallographic information and lay the foundation for calculating solid-state intergrowth unit energetics that are a prerequisite for mechanistic models. We also demonstrate how dimeric growth units can be produced, starting from this same strategy. We tested this approach on three molecular crystals with crystallography of varying degrees of complexicty (Z' = 0.5, 1, and 2, respectively) to demonstrate interpretation of crystallography. Our predicted crystal habits agreed favorably with experimental reports, where available, but more generally demonstrate the feasibility of this approach.

Ultimately, this software framework helps broaden the applicability of mechanistic modeling frameworks to more complex crystallography. Each type of chemical entity can be identified, regardless of whether these merely correspond to different spatial positions or are also chemically distinct; our ability to handle the latter enables interpretation of growth units for cocrystals, solvates, and organic salts, which would be even more prohibitive to describe via a case-by-case treatment related to the asymmetric unit. To implement mechanistic

models for cocrystals, solvates, and salts, appropriate mechanistic expressions must also account for multiple species in solution and distinct attachment rates for each species. However, modeling strategies for ionic crystal systems <sup>37,38</sup> have demonstrated the feasibility of such generalizations; coupled with a robust interpretation of the crystallography, application of mechanistic crystal growth models to such systems can now be considered.

### ASSOCIATED CONTENT

# **Supporting Information**

The Supporting Information is available free of charge at https://pubs.acs.org/doi/10.1021/acs.cgd.9b01105.

Solvent models, the PBCs, spiral shapes, detailed calculated results for crystals, and Appendices A, B, and C in this study (PDF)

## AUTHOR INFORMATION

## **Corresponding Author**

Michael F. Doherty — Department of Chemical Engineering, University of California, Santa Barbara, California 93106-5080, United States; orcid.org/0000-0003-3309-3082; Phone: +1 805-893-5309; Email: mfd@ucsb.edu

#### **Authors**

- Yongsheng Zhao Department of Chemical Engineering, University of California, Santa Barbara, California 93106-5080, United States; orcid.org/0000-0003-1224-1787
- Carl J. Tilbury Department of Chemical Engineering, University of California, Santa Barbara, California 93106-5080, United States; Occid.org/0000-0002-4736-1239
- Steven Landis Department of Electrical and Computer Engineering, University of California, Santa Barbara, California 93106-9560, United States
- Yuanyuan Sun Department of Chemical Engineering, University of California, Santa Barbara, California 93106-5080, United States
- Jinjin Li National Key Laboratory of Science and Technology on Micro/Nano Fabrication, Department of Micro/Nano Electronics, Shanghai Jiao Tong University, Shanghai 200240, China
- Peng Zhu Department of Chemical Engineering, University of California, Santa Barbara, California 93106-5080, United States; National Key Laboratory of Science and Technology on Micro/Nano Fabrication, Department of Micro/Nano Electronics, Shanghai Jiao Tong University, Shanghai 200240, China

Complete contact information is available at: https://pubs.acs.org/10.1021/acs.cgd.9b01105

#### **Notes**

The authors declare no competing financial interest.

## ACKNOWLEDGMENTS

The authors are grateful for the financial support provided by Eli Lilly and Company, Novartis, Pfizer, and the International Fine Particle Research Institute. The authors acknowledge support from the Center for Scientific Computing from the California NanoSystems Institute and Materials Research Laboratory: an NSF Materials Research Science and Engineering Center (Grant No. DMR-1720256) and NSF Grant No. CNS-1725797. We are indebted to Dr. S. M. Reutzel-Edens

(Eli Lilly) and Prof. S. L. Price (Univ. College London) for bringing the tazofelone-toluene crystal system to our attention.

#### REFERENCES

- (1) Li, J.; Tilbury, C. J.; Kim, S. H.; Doherty, M. F. A design aid for crystal growth engineering. *Prog. Mater. Sci.* **2016**, *82*, 1–38.
- (2) Variankaval, N.; Cote, A. S.; Doherty, M. F. From form to function: Crystallization of active pharmaceutical ingredients. *AIChE J.* **2008**, *54*, 1682–1688.
- (3) Yang, H. G.; Sun, C. H.; Qiao, S. Z.; Zou, J.; Liu, G.; Smith, S. C.; Cheng, H. M.; Lu, G. Q. Anatase TiO<sub>2</sub> single crystals with a large percentage of reactive facets. *Nature* **2008**, 453, 638.
- (4) Wu, C.; Xie, Y. Controlling phase and morphology of inorganic nanostructures originated from the internal crystal structure. *Chem. Commun.* **2009**, 5943–5957.
- (5) Winn, D.; Doherty, M. F. Modeling crystal shapes of organic materials grown from solution. *AIChE J.* **2000**, *46*, 1348–1367.
- (6) Burton, W.-K.; Cabrera, N.; Frank, F. The growth of crystals and the equilibrium structure of their surfaces. *Philos. T. R. Soc. A, Mathematical and Physical Sciences* **1951**, 243, 299–358.
- (7) Snyder, R. C.; Doherty, M. F. Predicting crystal growth by spiral motion. *Proc. R. Soc. London, Ser. A* **2009**, 465, 1145–1171.
- (8) Kuvadia, Z. B.; Doherty, M. F. Spiral growth model for faceted crystals of non-centrosymmetric organic molecules grown from solution. *Cryst. Growth Des.* **2011**, *11*, 2780–2802.
- (9) Tilbury, C. J.; Joswiak, M. N.; Peters, B.; Doherty, M. F. Modeling Step Velocities and Edge Surface Structures during Growth of Non-Centrosymmetric Crystals. *Cryst. Growth Des.* **2017**, *17*, 2066–2080.
- (10) Shim, H.-M.; Koo, K.-K. Molecular Approach to the Effect of Interfacial Energy on Growth Habit of  $\varepsilon$ -HNIW. *Cryst. Growth Des.* **2016**, *16*, 6506–6513.
- (11) Shim, H.-M.; Myerson, A. S.; Koo, K.-K. Molecular modeling on the role of local concentration in the crystallization of L-methionine from aqueous solution. *Cryst. Growth Des.* **2016**, *16*, 3454–3464.
- (12) Shim, H.-M.; Koo, K.-K. Crystal morphology prediction of hexahydro-1, 3, 5-trinitro-1, 3, 5-triazine by the spiral growth model. *Cryst. Growth Des.* **2014**, *14*, 1802–1810.
- (13) Steed, K. M.; Steed, J. W. Packing Problems: High Z' Crystal Structures and Their Relationship to Cocrystals, Inclusion Compounds, and Polymorphism. *Chem. Rev.* **2015**, *115*, 2895–2933.
- (14) Price, S. L. Predicting crystal structures of organic compounds. *Chem. Soc. Rev.* **2014**, *43*, 2098–2111.
- (15) van Eijck, B. P.; Kroon, J. Structure predictions allowing more than one molecule in the asymmetric unit. *Acta Crystallogr., Sect. B: Struct. Sci.* **2000**, *56*, *535*–*542*.
- (16) van de Streek, J.; Neumann, M. A. Crystal-structure prediction of pyridine with four independent molecules. *CrystEngComm* **2011**, *13*, 7135–7142.
- (17) Bond, A. D. Automated derivation of structural class symbols and extended Z' descriptors for molecular crystal structures in the Cambridge Structural Database. *CrystEngComm* **2008**, *10*, 411–415.
- (18) Day, G. M. Current approaches to predicting molecular organic crystal structures. *Crystallogr. Rev.* **2011**, *17*, 3–52.
- (19) Tilbury, C. J.; Doherty, M. F. Modeling layered crystal growth at increasing supersaturation by connecting growth regimes. *AIChE J.* **2017**, *63*, 1338–1352.
- (20) Tilbury, C. J.; Green, D. A.; Marshall, W. J.; Doherty, M. F. Predicting the Effect of Solvent on the Crystal Habit of Small Organic Molecules. *Cryst. Growth Des.* **2016**, *16*, 2590–2604.
- (21) Li, J.; Tilbury, C. J.; Joswiak, M. N.; Peters, B.; Doherty, M. F. Rate Expressions for Kink Attachment and Detachment During Crystal Growth. *Cryst. Growth Des.* **2016**, *16*, 3313–3322.
- (22) Macrae, C. F.; Edgington, P. R.; McCabe, P.; Pidcock, E.; Shields, G. P.; Taylor, R.; Towler, M.; van de Streek, J. Mercury: visualization and analysis of crystal structures. *J. Appl. Crystallogr.* **2006**, 39, 453–457.

- (23) Wang, J.; Wang, W.; Kollman, P. A.; Case, D. A. Automatic atom type and bond type perception in molecular mechanical calculations. *J. Mol. Graphics Modell.* **2006**, 25, 247–260.
- (24) Frisch, M. J.; Trucks, G. W.; Schlegel, H. B.; Scuseria, G. E.; Robb, M. A.; Cheeseman, J. R.; Scalmani, G.; Barone, V.; Mennucci, B.; Petersson, G. A.; Nakatsuji, H.; Caricato, M.; Li, X.; Hratchian, H. P.; Izmaylov, A. F.; Bloino, J.; Zheng, G.; Sonnenberg, J. L.; Hada, M.; Ehara, M.; Toyota, K.; Fukuda, R.; Hasegawa, J.; Ishida, M.; Nakajima, T.; Honda, Y.; Kitao, O.; Nakai, H.; Vreven, T.; Peralta, J. E.; Ogliaro, F.; Bearpark, M.; Heyd, J. J.; Brothers, E.; Kudin, K. N.; Staroverov, V. N.; Kobayashi, R.; Normand, J.; Raghavachari, K.; Rendell, A.; Burant, J. C.; Iyengar, S. S.; Tomasi, J.; Cossi, M.; Rega, N.; Millam, J. M.; Klene, M.; Knox, J. E.; Cross, J. B.; Bakken, V.; Adamo, C.; Jaramillo, J.; Gomperts, R.; Stratmann, R. E.; Yazyev, O.; Austin, A. J.; Cammi, R.; Pomelli, C.; Ochterski, J. W.; Martin, R. L.; Morokuma, K.; Zakrzewski, V. G.; Voth, G. A.; Salvador, P.; Dannenberg, J. J.; Dapprich, S.; Daniels, A. D.; Farkas, O.; Foresman, J. B.; Ortiz, J. V.; Cioslowski, J.; Fox, D. J. Gaussian 09, revision A. 02; Gaussian, Inc.: Wallingford, CT, 2009.
- (25) Brock, C. P.; Dunitz, J. D. Temperature dependence of thermal motion in crystalline naphthalene. *Acta Crystallogr., Sect. B: Struct. Crystallogr. Cryst. Chem.* **1982**, 38, 2218–2228.
- (26) Wang, J.; Wolf, R. M.; Caldwell, J. W.; Kollman, P. A.; Case, D. A. Development and testing of a general amber force field. *J. Comput. Chem.* **2004**, *25*, 1157–1174.
- (27) Grimbergen, R.; Reedijk, M.; Meekes, H.; Bennema, P. Growth behavior of crystal faces containing symmetry-related connected nets: a case study of naphthalene and anthracene. *J. Phys. Chem. B* **1998**, 102, 2646–2653.
- (28) Wells, A. XXI. Crystal habit and internal structure. *Philos. Mag.* **1946**, 37, 184–199.
- (29) Bravais, A. études Crystallographic; Gauthier-Villars: Paris, France, 1866.
- (30) Donnay, J. D. H.; Harker, D. A new law of crystal morphology extending the law of Bravais. *American Mineralogist: Journal of Earth and Planetary Materials* **1937**, 22, 446–467.
- (31) Friedel, G. Etudes sur la loi de Bravais. Bull. Soc. Fr. Mineral. 1907, 30, 326-455.
- (32) Hartman, P.; Bennema, P. The attachment energy as a habit controlling factor: I. Theoretical considerations. *J. Cryst. Growth* **1980**, 49, 145–156.
- (33) Feld, R.; Lehmann, M. S.; Muir, K. W.; Speakman, J. C. Z. Kristallogr. Cryst. Mater. 1981, 157, 157.
- (34) Berkovitch-Yellin, Z. Toward an ab initio derivation of crystal morphology. *J. Am. Chem. Soc.* **1985**, *107*, 8239–8253.
- (35) https://www.youtube.com/watch?v=4G6cFXtbwNo (accessed 2019-07-02).
- (36) Price, L. S.; McMahon, J. A.; Lingireddy, S. R.; Lau, S.; Diseroad, B. A.; Price, S. L.; Reutzel-Edens, S. M. A molecular picture of the problems in ensuring structural purity of tazofelon. *J. Mol. Struct.* **2014**, *1078*, 26–42.
- (37) Dandekar, P.; Doherty, M. F. A mechanistic growth model for inorganic crystals: Solid-state interactions. *AIChE J.* **2014**, *60*, 3707–3719.
- (38) Dandekar, P.; Doherty, M. F. A mechanistic growth model for inorganic crystals: growth mechanism. *AIChE J.* **2014**, *60*, 3720–3731.